Glycobiology vol. 7 no. 5 pp. 597–604, 1997

Molecular dynamics simulations of the two disaccharides of hyaluronan in aqueous solution

Andrew Almond[1], John K.Sheehan and Andy Brass

Division of Biochemistry, School of Biological Sciences, University of Manchester, Manchester M13 9PT, UK

[1]To whom correspondence should be addressed

Hyaluronan is an unusually stiff polymer when in aqueous solution, which has important consequences for its biological function. Molecular dynamics simulations of hyaluronan disaccharides have been performed, with explicit inclusion of water, to determine the molecular basis of this stiffness, and to investigate the dynamics of the glycosidic linkages. Our simulations reveal that stable sets of hydrogen bonds frequently connect the neighboring residues of hyaluronan. Water caging around the glycosidic linkage was observed to increase the connectivity between sugars, and further constrain them. This, we propose, explains the unusual stiffness of polymeric hyaluronan. It would allow the polysaccharide to maintain local secondary structure, and occupy large solution domains consistent with the visco-elastic nature of hyaluronan. Simulations in water showed no significant changes on inclusion of the exo-anomeric effect. This, we deduced, was due to hyaluronan disaccharides ordering first shell water molecules. In some cases these waters were observed to transiently induce conformational change, by breaking intramolecular hydrogen bonds.

Key words: conformation/hyaluronan/hydrogen bonds/molecular dynamics/water

Introduction

The glycosaminoglycan hyaluronan (HA) is a high molecular mass linear polysaccharide which is an important component of tissues such as the vitreous, Wharton's jelly and synovial fluid. It plays a key organizational role in the properties of many extracellular matrices, such as cartilage, through its interaction with proteins and proteoglycans. HA is also involved in the important processes of cell adhesion, proliferation and migration (Laurent and Fraser, 1992). It is unique among the glycosaminoglycans, being extruded directly from cell surfaces (Prehm, 1984), and carrying no sulfation. HA is a commercially important molecule, with considerable cosmetic and therapeutic application because it has good space-filling properties and is nonimmunogenic.

The HA polymer is built up from linear repeats of the disaccharide (-GlcNAc-β1,4-GlcA-β1,3-) where GlcA is β-D-glucuronic acid, and GlcNAc is β-D-N-acetylglucosamine. It is present throughout the extracellular matrix, with a size varying between 400 and 20,000 sugar units. Under physiological conditions it is a negatively charged polyelectrolyte, and physical studies indicate that it behaves as a stiff random worm-like coil (Cleland, 1984). At relatively low concentrations HA can form the basis of a visco-elastic solution. Its physical properties are strongly affected by the presence of cations. For example, the intrinsic viscosity increases with sodium concentration (Fouissac *et al.*, 1992).

X-Ray fiber diffraction has been used successfully to solve the solid state structure of HA in a number of cationic environments; left-handed 4-fold helices are found in sodium and potassium environments, and left-handed 3-fold helices in calcium (Sheehan and Atkins, 1983). Under acidic conditions an extended 2-fold helix is observed with most cations (Atkins *et al.*, 1972). Potassium and ammonium are exceptions, forming a left-handed 4-fold anti-parallel double helix (Sheehan *et al.*, 1977). All of these structures are consistent with the presence of intramolecular hydrogen bonds across the glycosidic linkages (Winter and Smith, 1975).

A variety of experimental evidence exists to support the presence of direct hydrogen bonds between adjacent sugars in solution, for example the relatively slow oxidation rate of HA by periodate (Scott and Tigwell, 1978). Variations of ^{1}H NMR chemical shifts in the spectra of HA in DMSO (Scott *et al.*, 1981, 1984; Heatley *et al.*, 1982) provided direct evidence for intramolecular hydrogen bonds, at least in DMSO. Based on these results, x-ray data (Atkins *et al.*, 1972) and computer modeling, a 2-fold helical structure was proposed (Atkins *et al.*, 1980) for HA in DMSO incorporating four intramolecular hydrogen bonds per disaccharide. The suggested sets of hydrogen bonds are shown in Figure 1. This picture is supported to some extent by preliminary computer simulations (Scott *et al.*, 1991). It is possible, therefore, that intramolecular hydrogen bonding could contribute to some of the atypical structural and rheological properties of HA. However, the exact microscopic basis of these characteristics is poorly understood.

Structural information on HA is available in the solid state, and when solvated in DMSO. However, structural data for HA in water, as is the case for carbohydrates in general, is scarce. A reason for this situation is the inability to observe exchangeable hydroxyl protons in the ^{1}H NMR spectra of carbohydrates in aqueous solution under normal conditions. Therefore, in this article we have used molecular dynamics (MD) simulation to gain insights into the conformation and dynamics of hydrated HA. Although MD simulations cannot by themselves provide direct structural information, they can be used to generate hypotheses which can be tested experimentally.

The MD simulations have been used to address a number of key questions regarding the structure and function of hydrated HA. Firstly, are the hydrogen bonds between adjacent sugar residues proposed to exist in DMSO present in water, and if so how persistent are they? Secondly, what is the microscopic basis for the atypical stiffness of the hyaluronan polymer? Thirdly, how does the presence of water affect the structure and dynamics of HA?

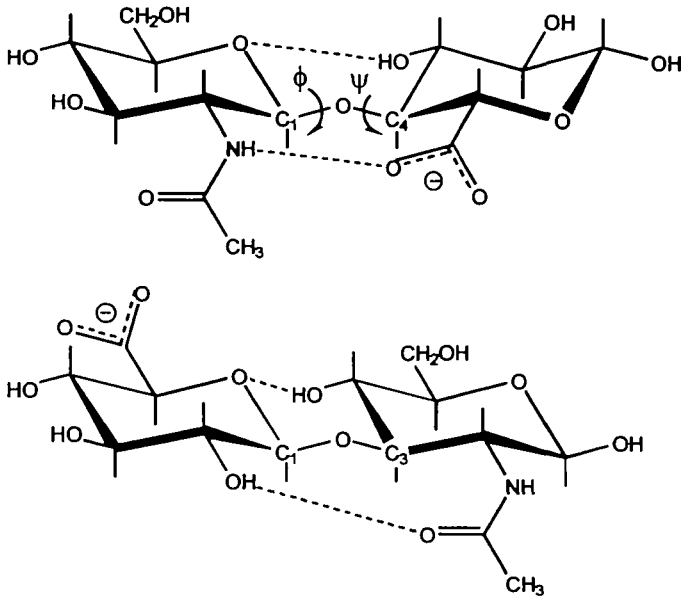

Fig. 1. The two disaccharides of hyaluronan, β1,4 linked (top), and β1,3 linked (bottom) showing the proposed intramolecular hydrogen bonds.

Results

(ϕ,ψ) glycosidic angles were extracted for each frame, using the angular definitions given in *Materials and methods* section. The occurrence of pairs of dihedral angles was calculated by accumulating them into bins at 6° intervals. Using the total number of frames in the simulation we could calculate the probability of pairs of (ϕ,ψ) arising. Assuming that we had explored a good percentage of the total number of possible conformations, we can estimate the energy of each (ϕ,ψ) conformation by relating probability to the Boltzmann energy (Mandl, 1988) of that state. Contours were then calculated to reconstruct the Ramachandran-like energy map for each linkage. For the vacuum case (Figure 2) these agreed well with adiabatic grid searches (see, for example, Brady and Schmidt, 1993) we calculated. These maps allowed us to compare the exploration of disaccharides under differing simulation conditions. Figure 2 (top right and bottom left) shows the energy contour plots for a β1,4 linkage simulated in water, with and without exo-anomeric parameters. Firstly, we noticed that the same region was explored in both cases. Secondly, the minimum energy in ϕ corresponded to +60° in both cases, consistent with the exo-anomeric effect. Therefore, we concluded that inclusion of exo-anomeric parameters in our solvated simulations had no significant effect.

We calculated the percentage of total time that hydrogen bonds connected adjacent sugar residues of the two different disaccharides. Simulations used only unmodified CHARMm version 22 parameters. Figure 3 shows these results averaged over 500 ps simulations in water and vacuum (shown in parentheses). We observed three hydrogen bonds to be well maintained across a β1,4 linkage; O3(g)-HO3 →O5(n), N(n)-HN → O6(g), O6(n)-HO6 → O3(g), and three across a β1,3 linkage; O4(n)-HO4 → O5(g), O2(g)-HO2 → O7(n), O4(n)-HO4 → O6(g), where (n) specifies the GlcNAc residue and (g) is the GlcA residue. Both the persistence and the total time of intramolecular hydrogen bonding was observed to increase in water. The enhanced persistence of hydrogen bonds would be consistent with bulk solvent constraining molecular motion, allowing groups to remain adjacent for longer periods. However, we would not intuitively expect an enhancement of the total time, as water molecules are thought to compete for the hydrogen bonds (Scott *et al.*, 1984).

We considered the overall effect of water on HA by comparing the dynamics of glycosidic linkages in water and in vacuum. Figure 4 shows the autocorrelation function for the ϕ torsional angle of a β1,4 linked disaccharide in vacuum. To understand the type of motion characterized by this function, we attempted to model the glycosidic linkage in vacuum. To a first approximation the motion is described by a harmonic oscillator (Main, 1978) subject to viscous damping and driven by stochastic noise, which effectively places the system in a heat bath. Assuming θ is the angular deviation of a linkage from its mean position, then Equation 1 represents the equation of motion. ω_0 is a measure of the natural frequency of oscillation about θ, and γ indicates the rate of energy dissipation by long range nonbonded interactions.

$$\frac{d^2\theta}{dt^2} + \gamma \frac{d\theta}{dt} + \omega_0^2\theta = F(t) \qquad (1)$$

We calculated the autocorrelation functions for the ϕ and ψ torsions of both disaccharides in vacuum. The autocorrelation function of θ was fitted to each by adjusting the values of γ and ω_0 systematically. When $\omega_0 = 4.7\ ps^{-1}$ and $\gamma = 2.3\ ps^{-1}$ we found a good fit to ϕ of a β1,4 linkage (Figure 4). Therefore, the period of oscillation about this bond is 1.4 ps. Similarly for ϕ of a β1,3 linkage, $\omega_0 = 3.9\ ps^{-1}$ and $\gamma = 1.7\ ps^{-1}$ produced the best fit, corresponding to a period of oscillation of 1.7 ps. Since the period of oscillation about a bond is inversely proportional to its stiffness, we deduced that the β1,4 is slightly stiffer than the β1,3 linkage in vacuum. It should be noted that the ψ torsional motions also fitted into this scheme, although not as agreeably.

When we included water in our simulations the dynamics we observed changed considerably. The autocorrelation functions for ϕ and ψ dropped sharply over a short time and then decayed exponentially. Similar results have been extracted from simulations of maltose (Brady and Schmidt, 1993), and cellobiose (Hardy and Sarko, 1993). Figure 5 shows the autocorrelation function for ϕ of a β1,4 linked disaccharide in water. The lack of oscillation and slow decay of the correlation function is indicative of highly overdamped motion. However, we could not model the system using the damped simple harmonic oscillator described above, where the overdamped autocorrelation function had only one exponential component. Instead we fitted an exponential to the latter part of the correlation function (Figure 5). From this we calculated the relaxation time of the motion to be 1.6 ps. For comparison, the relaxation time of water molecules is approximately 10 ps at 300K. It would appear that glycosidic torsional motions in water involve two processes. A fast process, which we assume relates to transfer of momentum between saccharide residues, and a slow process relating to the interaction with water.

Specific interactions with water molecules were clear when we investigated water bridges (Figure 6) between polar sugar groups, particularly around the glycosidic linkage. Figure 7 shows the frequency of single water molecules bridging the glycosidic linkage of each disaccharide, extracted from simulation. Our simulations revealed that groups could be bridged by water molecules for up to 40% of the total time. All groups

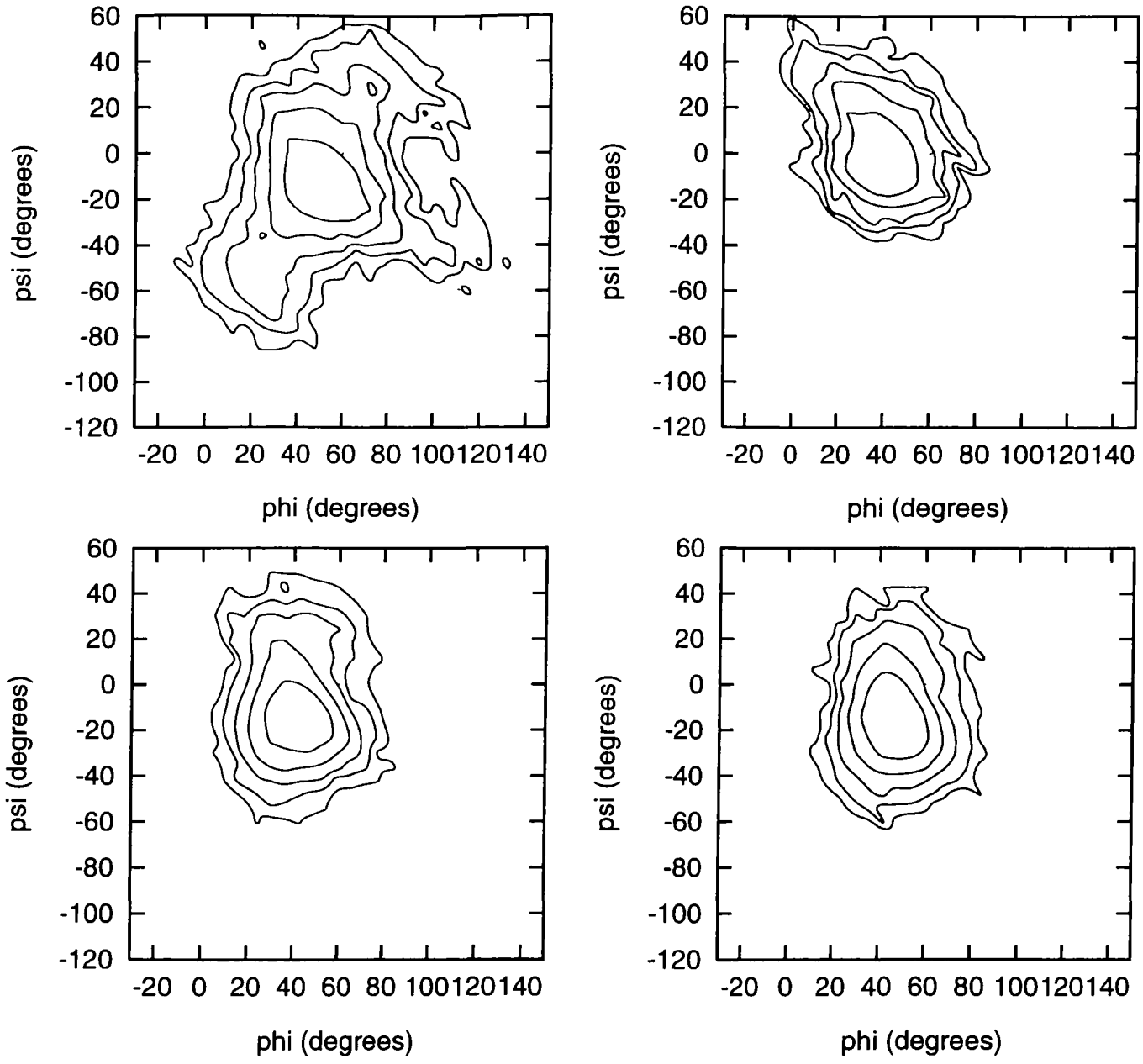

Fig. 2. Contour plots calculated from molecular dynamics simulations. Contours are drawn at 17, 33, 50, 67, and 83% of the highest energy state. Top left, CHARMm 22 parameters used to simulate the β1,4 disaccharide in vacuum (500 ps). Top right, Exo-anomeric corrected potential used to simulate a β1,4 disaccharide in water (150 ps). Bottom left, CHARMm22 parameters used to simulate a β1,4 disaccharide in water (500 ps). Bottom right; same, but for β1,3 disaccharide.

involved in intramolecular hydrogen bonding were observed to participate in forming these water bridges.

Over a simulation many different water molecules were observed to bridge a particular pair of groups, changing by diffusion. To study this process we gave each water in the simulation (1000 in total) a specific number. We chose pairs of polar groups which we had previously observed to be involved in water bridging. Then, for each frame that a water bridged these groups we recorded its identification number. Figure 9 details some identification numbers of water hydrogen bonding to both O5(n) and O3(g) at the β1,4 linkage, over 200 ps. Between 340 ps and 390 ps a water can be seen to be resident in this location (marked by an arrow). Residence times between 30 and 50 ps were observed quite frequently, describing the typical time of water rearrangements.

Bridges involving two water molecules were also seen frequently. In most cases these bridges were observed between the same groups as the single water case. There are two important exceptions. Across a β1,4 linkage O6(n) was seen to be linked to O2(g), and across a β1,3 linkage O7(n) was seen to be linked to O3(g). Although water was continually diffusing in and out of residence, on average we could identify the presence of a structured first water shell. This resulted in the linkage region being surrounded by a water cage which actually complemented the sets of intramolecular hydrogen bonds. Therefore, even though water was competing for the intramolecular hydrogen bonds, it increased the connectivity of neighboring sugar residues. In this way the linkage effectively increased in stiffness.

Figure 8 shows the trajectory of the ψ dihedral angle for a

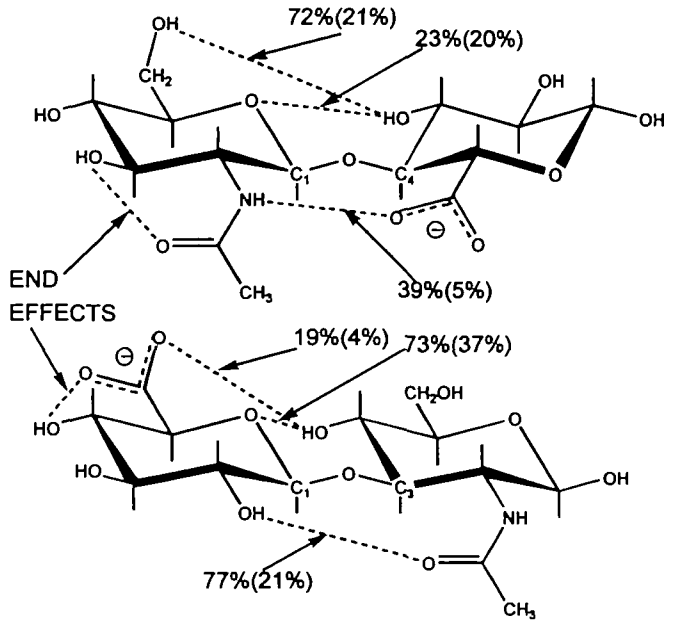

Fig. 3. Probability of each of the intramolecular hydrogen bonds being formed during 500 ps simulations in water, for β1,4 linkage (top) and β1,3 linkage (bottom). Numbers in parentheses are similar results from vacuum simulations.

β1,4 linkage. Noticeably ψ migrates from its minima (0°) at intervals of approximately 200 ps. Plotted along the top of Figure 8 is a trace detailing hydrogen bonding between O6(n)-OH6 and O3(g). A clear correlation exists between absence of this intramolecular hydrogen bond and migrations of ψ. We observed that this lack of hydrogen bonding between these groups was due to a long-lived water bridging them. The water was seen to completely break this hydrogen bond for a period of about 30 ps. Figure 10 shows a typical position for this water. It should be noticed that the water is forming hydrogen bonds to both hydroxyl O3(g) and hydroxymethyl OH6(n). The hydroxymethyl group has not previously been attributed a function in HA, making this an interesting finding. We also

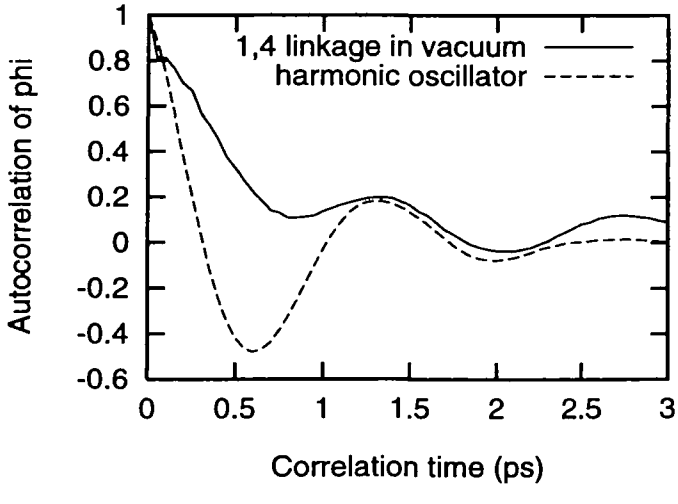

Fig. 4. Correlation function for rotations about the ϕ bond of a β1,4 linked disaccharide in vacuum. Also shown is the theoretical correlation function for a damped simple harmonic oscillator with $\omega_0 = 4.7$ ps^{-1} and $\gamma = 2.3$ ps^{-1} (see text).

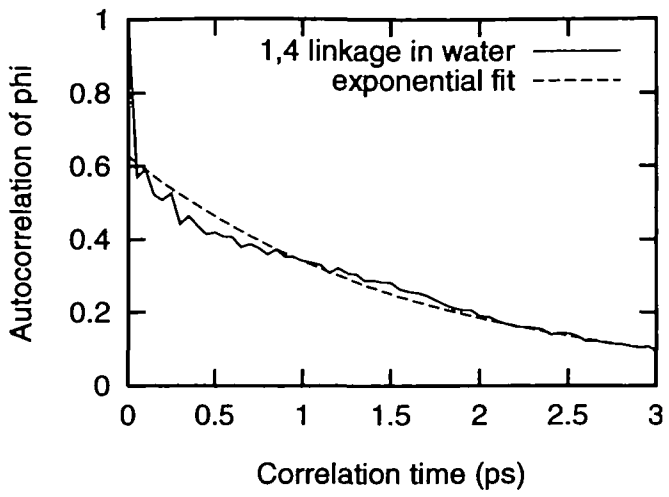

Fig. 5. Correlation function for rotations about the ϕ bond of a β1,4 linked disaccharide in water. An exponential fit has been made to the latter part of the correlation function, having the equation 0.628 exp (–0.613t).

found that the acetamido torsion (H2-C2-N-HN) could undergo unusual transition. Interchange between the *trans* and *cis* state of the acetamido torsion of a β1,4 disaccharide (Figure 11) can been attributed to water structuring. In the *trans* structure (predominant) a water was seen to bridge N(n) and O6(g), and in the *cis* structure a water was seen to bridge N(n), O6(g) and O4(g), the glycosidic oxygen. In the latter case the water was observed to be detached from bulk solvent by forming hydrogen bonds to the solute.

Discussion

Our simulations have been performed on disaccharides, the smallest units of HA. Although they possess large end effects, insights can be gained into the dynamics of the two linkages of HA. We have observed no marked differences in the flexibility of β1,3 and β1,4 linkages in TIP3P water (Figure 2). This has been concluded from other MD simulations of HA (Holmbeck *et al.*, 1994). However, ^{13}C NMR showed larger chemical shifts associated with the β1,3 than the β1,4 linkage (Cowman *et al.*, 1996). This was interpreted as the β1,3 linkage having a greater conformational flexibility. However, an alternative explanation was given. Rotation of the acetamido group at C2 could substantially affect the electrostatic environment around the β1,3 linkage. Based on our simulations the latter explanation seems likely, since we observed the acetamido torsion to be conformationally flexible (Figure 11).

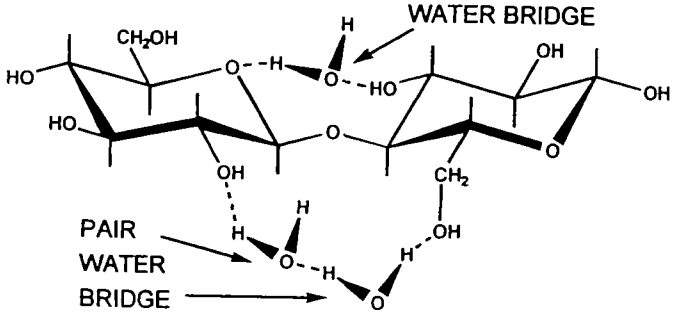

Fig. 6. Illustration of the two different types of water bridges studied.

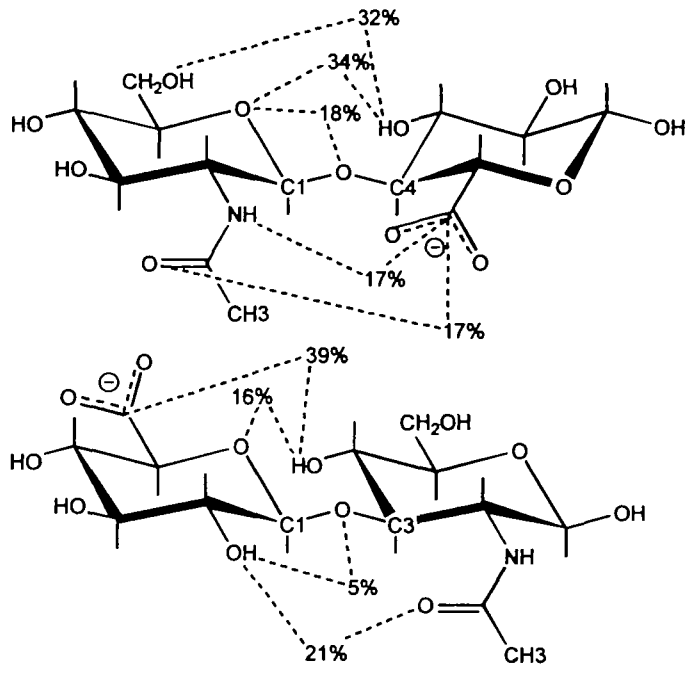

Fig. 7. Probability of each of the intramolecular hydrogen bonds being formed during 500 ps simulations in water, for β1,4 linkage (top) and β1,3 linkage (bottom).

At the simplest level rotation about a bond results from its harmonic potential, as a consequence of surrounding groups staggering and eclipsing each other. The fact that we could model the glycosidic linkage in vacuum by a harmonic oscillator indicates that a similar situation exists here. Therefore, the results of simulations in vacuum would be expected to be particularly sensitive to the rotational potential defined at the glycosidic bonds. It would appear that careful consideration of these parameters is a necessity when performing vacuum simulations. In water, however, we observed no significant differences when we included the exo-anomeric effect. The overdamped nature of the autocorrelation function for ϕ indicated

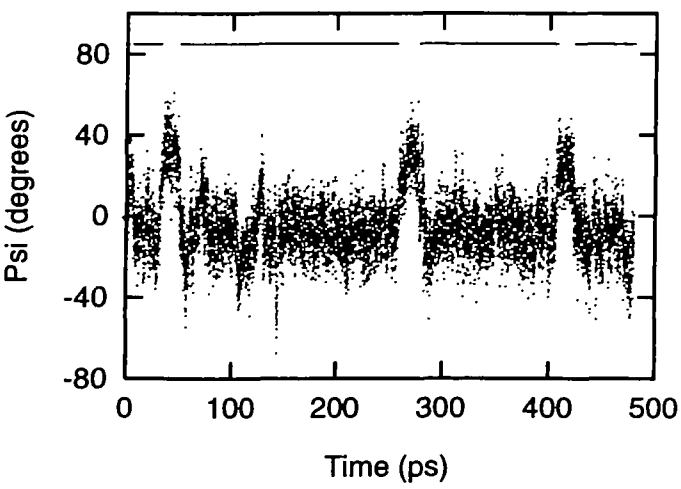

Fig. 8. Correlation between periodic motions in ϕ and intramolecular hydrogen bonding between O6(n)-OH6 → O3(g), during a 500 ps simulation of a β1,4 linked disaccharide in water. Each frame for which a direct hydrogen bond was found is marked along the top of the plot.

that the interaction with water was a much more important consideration. Effects due to slight adjustment of the bond rotational potential were totally concealed by placing the molecules in water. We observed water molecules to be frequently resident in the region of the glycosidic oxygen. These waters, we propose, would have two important consequences for the glycosidic linkages of HA. Firstly, to constrain each linkage by forming bridges across it. Secondly, to reduce the n(O)→ σ(CO) electron interactions (Thogerson *et al.*, 1982) thought to be responsible for the exo-anomeric effect. Therefore, we conclude that inclusion of the exo-anomeric effect into water simulations, by the method described here, does not significantly affect the dynamics of HA glycosidic linkages.

We believe that local rigidity in HA is affected by a combination of intramolecular hydrogen bonds and water caging around them. Two hydrogen bonds are seen per disaccharide in x-ray fiber refinements, and four are proposed for HA in DMSO by NMR. However, we have observed up to six in our simulations (three across each linkage). This favorable array of hydrogen bonds is possible due to the substituents on HA being equatorial. It is thought that in polymeric HA sets of hydrogen bonds run down its length, stiffening the chain (Scott, 1989). The hexosamine residues are crucial, since the acetamido moieties can act as both acceptors and donors of hydrogen bonds in opposite directions. Uronic acid residues are instrumental in introducing a charge density into the molecule. Chondroitin sulfates have structures resembling HA, lacking only the hydrogen bond between the C4 hydroxyl group of the hexosamine and the ring oxygen of the neighboring uronic acid residue. They would thus be expected to have a similar rigidity. Other glycosaminoglycans have less favorable interactions across their glycosidic linkages, for example in dermatan sulfate. Therefore, a relationship could exist between ability to form these hydrogen bonded arrays and their uses. Both HA and chondroitin-4-sulfate commonly perform space filling roles in the extracellular matrix. Also, intramolecular hydrogen bonds provide resistance against chemical attack, which could be an important attribute of a structural molecule. This is consistent with the slow rate of periodate oxidation found for HA and chondroitin-4-sulphate (Scott and Tigwell, 1978). HA is the molecule responsible for noncovalent organization of proteoglycans, by binding irreversibly to link protein. It is thought that a decasaccharide region of HA is required for attachment to the aggrecan G1 binding domain (Hardingham and Fosang, 1992). Our results suggest that over this length the HA molecule would be relatively inflexible.

NMR is unable to probe the key hydroxyl groups in water because of rapid proton exchange under normal conditions (Poppe and Van Halbeek, 1994). However, the GlcNAc amide proton of HA is readily accessible. NMR in DMSO assigned down-field shifts to this proton resonance (Scott *et al.*, 1981). Conversely, in H_2O up-field shifts were observed (Cowman *et al.*, 1984). This suggested the existence of hydrogen bonds in DMSO, and lack of hydrogen bonds in water. Additional NMR studies showed that addition of water to HA solvated in DMSO significantly affected the environment around the amide proton (Heatley and Scott, 1988). This was interpreted as resulting from a water molecule bridging, and breaking, the hydrogen bond between amide proton and carboxylate group. Further support for this hypothesis was the increased HA chain mobility observed on exchanging the solvent from DMSO to H_2O (Cowman *et al.*, 1996). Other recent spectroscopic studies have found evidence for strong interaction between HA and water,

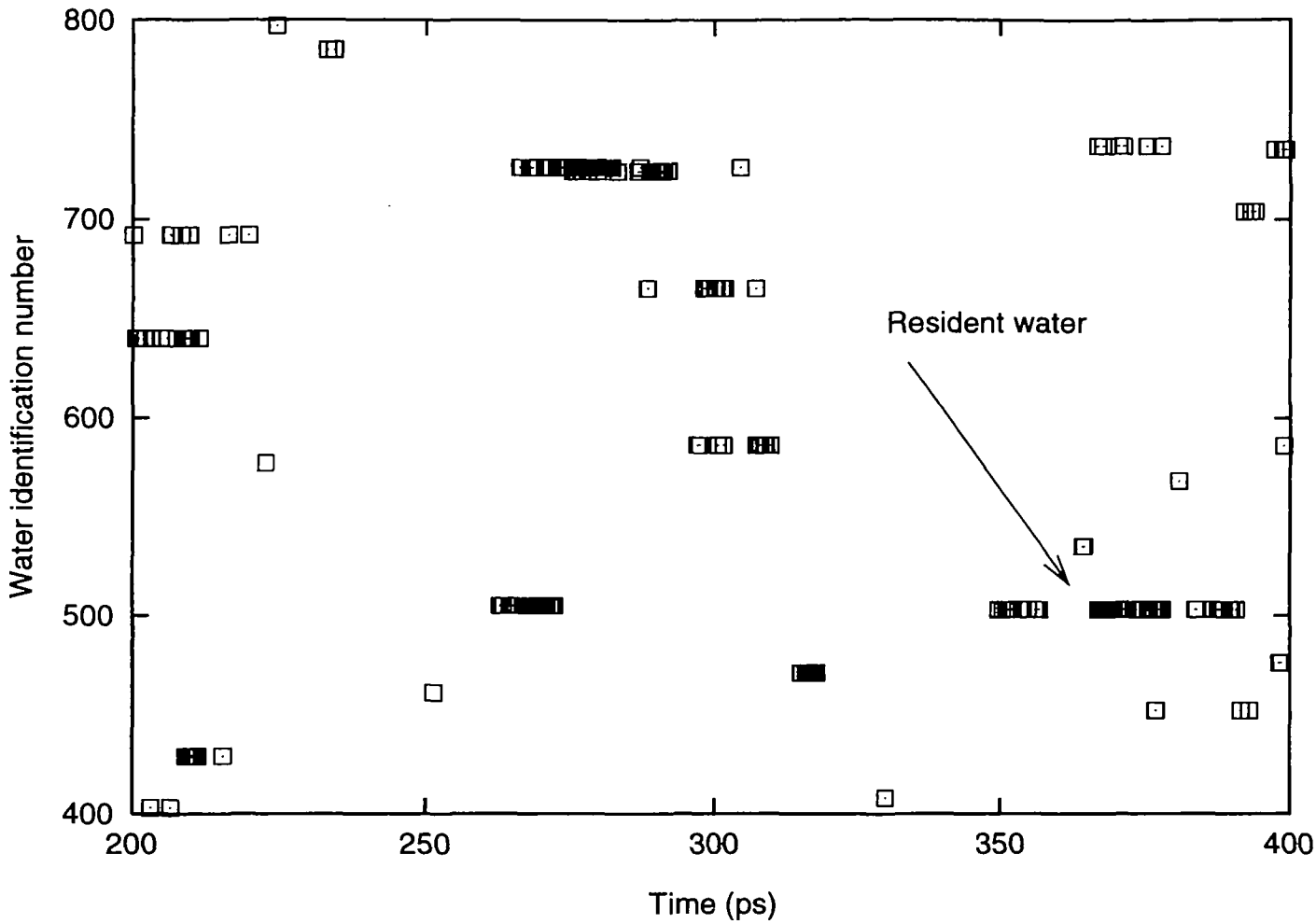

Fig. 9. Code numbers of waters bridging the two groups O5(n) and O3(g) at the β1,4 linkage, extracted from a 500 ps simulation in water.

but have failed to observe intramolecular hydrogen bonds in aqueous solution (Sicinska *et al.*, 1993). To consolidate these results we propose the following. Firstly, the bulk effects of solvent prolong intramolecular hydrogen bonds. This explains the strong intramolecular hydrogen bonding observed in DMSO. Secondly, as the polarity of the solvent increases these hydrogen bonds are competed for more frequently, reducing their total interaction time and therefore relaxing the chain. This explains the increase in mobility of the HA chain when exchanged from DMSO and into water solvent.

Space-filling models of HA suggested that a single water molecule could bridge the β1,4 linkage between acetamido and carboxylate groups (Heatley and Scott, 1988). The high H2-NH coupling constant (9–10 Hz) for the amide proton is apparently consistent with either a *cis* or *trans* conformation (Scott *et al.*, 1984), assigned with a relationship derived for peptide amide protons (Bystrov *et al.*, 1973). We most frequently observed the amide proton to be about 40° from *trans* to H2, consistent with a direct hydrogen bond to the carboxylate group. However, this did not preclude simultaneous water bridging between these groups. Only in a small number of cases did we observe a water molecule actually break a hydrogen bond (see Figure 10). When this occurred it had the potential to cause conformational change. The *cis* conformation of the amide proton that we observed is a specific example of this. Similar results have been observed in molecular dynamics studies of neocarrabiose in solution (Ueda and Brady, 1996).

Bridging between OH6(n) and O3(g) at a β1,4 linkage was observed to result in dramatic conformational changes of ψ lasting tens of picoseconds. Amazingly these occurred only approximately every 200 ps, much longer than the average time of water rearrangements (30 ps). Long simulations times are thus required in water to sample such conformations. Fluctuations of ψ would significantly affect the polymer thermodynamics of HA, and its nonspecific interactions within the extracellular matrix.

If waters are in specific association with the HA molecule, they may be an integral part of its molecular shape as felt by other molecules in the extracellular matrix. Water has been found to be incorporated into the structure of bound saccharides, for example concanavalin A complexed with methyl α-D-mannose (Naismith *et al.*, 1994). However, removal of water molecules could act as an effective energy barrier to binding if it is the naked polysaccharide that is recognized.

The most recent ^{13}C NMR studies have considered aqueous HA in different cationic environments (Sicinska and Lerner, 1996; Cowman *et al.*, 1996). They concluded that, on addition of salt, the observed differences in linkage mobility are not consistent with a simple electrostatic interaction. It appears that an acceptable understanding of HA may only be possible by

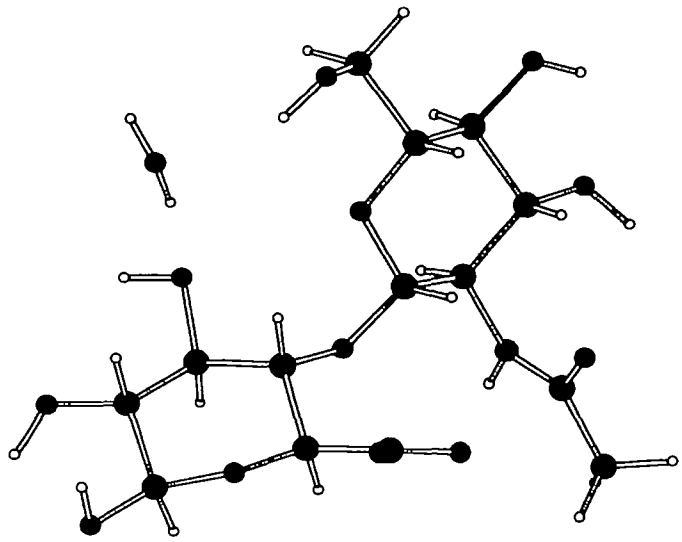

Fig. 10. Schematic drawing of a β1,4 linked disaccharide showing a water molecule bridging two groups, and resulting in the breaking of an intramolecular bond.

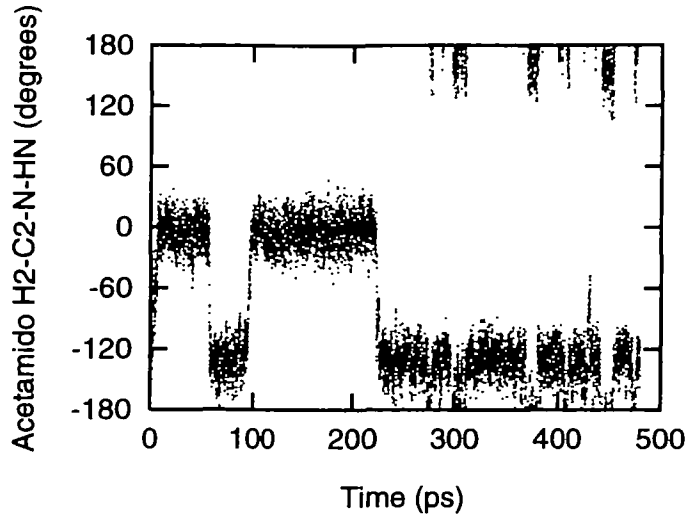

Fig. 11. History of the acetamido dihedral angle on the GlcNAc residue of a β1,4 linked disaccharide, from a 500 ps simulation in water.

including the counter-ion. However, this is difficult with the present force fields and computer power.

Conclusion

We have performed relatively long molecular dynamics simulations of HA disaccharides in aqueous solution. The simulations reveal that stable sets of hydrogen bonds frequently coupled the neighboring residues of HA. Water molecules were observed to increase their connectivity, and enhance the stiffness of linkages. This, we propose, is the microscopic basis for the unusual stiffness of the HA polymer.

Additionally, our simulations have shown that HA can order first shell water molecules. This indicates that water is involved in HA binding events. Water was also observed to introduce conformational transition states into the dynamics of HA linkages. These states, facilitated by water molecules bridging hydrogen bonding moieties, would be important in HA mediated interactions. For example, they could allow a receptor to uniquely recognize HA.

Admittedly, MD simulations cannot provide direct structural information. However, our simulations have generated hypotheses which can be tested experimentally. We are presently undertaking some of these experiments.

Materials and methods

All simulation work was performed with the molecular mechanics program CHARMm (Brooks *et al.*, 1983). The force field used by CHARMm is parameterized on the basis of experimental data for proteins and nucleic acids. Development of a suitable force field for carbohydrates has been hampered by a lack of experimental data. However, several attempts have appeared in recent years. The CHARMm force field has been modified to model maltose (Ha *et al.*, 1988) in vacuum. In this parameterization no special treatment of the glycosidic linkage was attempted. A number of observations have indicated that the glycosidic linkage is a nontypical C-O-C situation. Two of the four atoms bonded to the anomeric carbon atom are more electronegative than carbon, and have lone pair electrons. Electron transfer, which is inevitable, is thought to reduce the glycosidic bond lengths and perturb their rotational potential (Jeffrey *et al.*, 1978). Using the glycosidic torsional definitions adopted by other authors (Homans, 1990; Brady and Schmidt, 1993), namely, ϕ (H1-C1-Ox-Cx*) and ψ (C1-Ox-Cx*-Hx*), see Figure 1. For an α-D-glycoside the minimum in ϕ is in the region of –60°, and for a β-D-glycoside it is +60° (Tvaroska and Tomas, 1989). This phenomenon is termed the exo-anomeric effect. *Ab initio* data for the rotation in C-O-C-O type linkage has been parameterized into the AMBER scheme (Homans, 1990). Conveniently, the AMBER is directly compatible with the CHARMm force field.

It is not directly evident as to what effect, if any, slight modifications to the carbohydrate potential have when explicit solvent is included in simulations. To investigate this we initially performed 150 ps simulations of the β1,4 linked hyaluronan disaccharide including explicit solvent. In one case we used a parameter set with inclusion of the exo-anomeric effect (Homans, 1990), and in the second we used ordinary CHARMm version 22 parameters.

Calculations were carried out using the leap-frog formulation (Hockney, 1970) of the Verlet algorithm (Verlet, 1967), and hydrogen covalent bond lengths kept constant by applying the SHAKE procedure (van Gunsteren and Berendsen, 1977). This allowed an integration step size of 1 fs to be used with excellent precision. Although some force fields contain a specific term to represent hydrogen bonding, we modeled this interaction by appropriate atomic partial charges and van der Waals parameters for the hydrogen bond donor and acceptor atoms (Brady and Schmidt, 1993). Molecules were placed in 32 Å cubic water boxes, filled with 1000 TIP3P previously equilibrated water molecules (Jorgensen *et al.*, 1983), consistent with an initial molar concentration of 0.05 M. Nonbonded lists were generated using the grid search cubing algorithm, and updated every 20 steps. Edge effects were overcome by implementing periodic boundary conditions, and the nonbonded cut-off was set at 12 Å and reduced to zero by using the shifting function (Steinbach and Brooks, 1994). Each molecule was placed at the center of the box in the minimum energy conformation found from an adiabatic grid search. Any water molecules overlapping the solute were deleted. This starting configuration was subjected to 1000 steps of adopted basis Newton-Raphson minimization. Equilibration consisted of 40 ps during which the system was coupled to a heat bath at 300K, followed by 10 ps of adiabatic dynamics. During subsequent free dynamics system coordinates were written at 0.05 ps intervals.

For analysis purposes we extended the length of simulation. In view of our findings (see *Results*), we used only the unmodified CHARMm version 22 force field. 500 ps simulations were calculated for both the β1,3 and β1,4 linked disaccharides of hyaluronan in solution. We also performed the same simulations in vacuum using a constant dielectric of $80\epsilon_0$.

Structuring at the glycosidic linkage was considered by studying intramolecular hydrogen bonding. A hydrogen bond is defined as being made if the distance D (hydrogen donor) to A (hydrogen acceptor) is less than 3.5 Å and the angle D-H . . . A is less than 60°. At each frame in the simulation (9600 in total) every pair of polar groups was checked for direct hydrogen bonding, and an entry made in a table for any occurrence. This took the form of a 13 by 13 matrix for each disaccharide. From the totals the percentage of hydrogen bonding between any two groups could be calculated for the whole simulation. To indicate specific interactions with solvent a similar calculation was made detailing water bridging. Water bridging is defined here when two polar sugar groups are connected by a network involving n water molecules (Figure 6). For n larger than 2 it was found that virtually every group could be linked to every other, a limit set by the size of the solute. Therefore, only the cases of single

and pair water bridges were considered, and two separate tables were constructed per simulation for the two different cases.

Acknowledgment

Financial support for this work was provided by the Wellcome Trust.

Abbreviations

DMSO, dimethyl sulfoxide; GlcA, β-D-glucuronic acid; GlcNAc, β-D-N-acetylglucosamine; HA, hyaluronan; MD, molecular dynamics; NMR, nuclear magnetic resonance.

References

Atkins,E.D.T., Phelps,C.F. and Sheehan,J.K. (1972) The conformation of the mucopolysaccharides: hyaluronates. *Biochem. J.*, **128,** 1255–1263.

Atkins,E.D.T., Meader,D. and Scott,J.E. (1980) Model of hyaluronic acid incorporating four intramolecular hydrogen bonds. *Int. J. Biol. Macromol.*, **2,** 318–319.

Brady,J.W. and Schmidt,R.K. (1993) The role of hydrogen bonding in carbohydrates: molecular dynamics simulations of maltose in aqueous solution. *J. Phys. Chem.*, **97,** 958–966.

Brooks,B.R., Bruccoleri,R.E., Olafson,B.D., States,D.J., Swaminathan,S. and Karplus,M. (1983) CHARMm: a program for macromolecular energy minimization and dynamics calculations. *J. Comp. Chem.*, **4,** 187–217.

Bystrov,V.F., Ivanov,V.T., Portnova,S.L., Balashova,T.A. and Ovchinnikov,Y.A. (1973) Refinement of the angular dependence of the peptide vicinal NH-C$^{\alpha}$H coupling constant. *Tetrahedron*, **29,** 873–877.

Cleland,R.L. (1984) Viscometry and sedimentation equilibrium of partially hydrolyzed hyaluronate: comparison with theoretical models of worm-like chains. *Biopolymers*, 23, 647–666.

Cowman,M.K., Cozart,D., Nakanishi,K. and Balazs,E.A. (1984) ^{1}H NMR of glycosaminoglycans and hyaluronic acid oligosaccharides in aqueous solution: the amide proton environment. *Arch. Biochem. Biophys.*, **230,** 203–212.

Cowman,M.K., Hittner,D.M. and Feder-Davis,J. (1996) ^{1}C NMR studies of hyaluronan: conformational sensitivity to varied environments. *Macromolecules*, **29,** 2894–2902.

Fouissac,E., Milas,M., Rinaudo,M. and Borsali,R. (1992) Influence of the ionic strength on the dimensions of sodium hyaluronate. *Macromolecules*, **25,** 5613–5617.

Ha,S.N., Giammona,A., Field,M. and Brady,J.W. (1988) A revised potential energy for molecular mechanics studies of carbohydrates. *Carbohydr. Res.*, **180,** 207–221.

Hardingham,T.E. and Fosang,A.J. (1992) Proteoglycans: many forms and many functions. *FASEB J.*, **6,** 861–870.

Hardy,B.J. and Sarko,A. (1993) Molecular dynamics simulation of cellobiose in water. *J. Comp. Chem.*, **14,** 848–857.

Heatley,F. and Scott,J.E. (1988) A water molecule participates in the secondary structure of hyaluronan. *Biochem. J.*, **254,** 489–493.

Heatley,F., Scott,J.E., Jeanloz,R.W. and Walker-Nasir,E. (1982) Secondary structure in glycosaminoglycuronans: NMR spectra in dimethyl sulphoxide of disaccharides related to hyaluronic acid and chondroitin sulphate. *Carbohydr. Res.*, **99,** 1–11.

Hockney,R.W. (1970) The potential calculation and some applications. *Methods Comp. Phys.*, **9,** 135–211.

Holmbeck,S.M.A., Petillo,P.A. and Lerner,L.E. (1994) The solution conformation of hyaluronan: a combined NMR and molecular dynamics study. *Biochemistry*, **33,** 14246–14255.

Homans,S.W. (1990) A molecular force field for the conformational analysis of oligosaccharides: comparison of theoretical and crystal structures of Manα1–3Manα1–4GlcNAc. *Biochemistry*, **29,** 9110–9118.

Jeffrey,G.A., Pople,J.A., Binkley,J.S. and Vishveshwara,S. (1978) Application of *ab initio* molecular orbital calculations to the structural moieties of carbohydrates. *J. Am. Chem. Soc.*, **100,** 373–379.

Jorgensen,W.L., Chandrasekhar,J., Madura,J.D., Impey,R.W. and Klein,M.L. (1983) Comparison of simple potential functions for simulating liquid water. *J. Chem. Phys.*, **79,** 926.

Laurent,T.C. and Fraser,J.R.E. (1992) Hyaluronan. *FASEB J.*, **6,** 2397–2404.

Main,I.G. (1978) *Vibrations and Waves in Physics.* Cambridge University Press, London.

Mandl,F. (1988) *Statistical Physics,* Second edition. Wiley, Chichester.

Naismith,J.H., Emmerich,C., Habash,J., Harrop,S.J., Helliwell,J.R., Hunter,W.N., Raftery,J., Kalb,A.J. and Yariv,J. (1994) Refined structure of concanavalin a complexed with methyl α-D-mannopyranoside at 2.0 Å resolution and comparison with the saccharide-free structure. *Acta Crystallogr.*, **D50,** 847–858.

Poppe,L. and Van Halbeek,H. (1994) NMR spectroscopy of hydroxyl protons in supercooled carbohydrates. *Nature Struct. Biol.*, **1,** 215–216.

Prehm,P. (1984) Hyaluronate is synthesised at plasma membranes. *Biochem. J.*, **220,** 597–600.

Scott,J.E. (1989) Secondary structures in hyaluronan solutions: chemical and biological implications. In Laurent,T.C. (ed.), *The Biology of Hyaluronan.* Ciba Foundation Symposium 143. John Wiley, Chichester, U.K., pp. 6–20

Scott,J.E. and Tigwell,M.J. (1978) Periodate oxidation and the shapes of glycosaminoglycuronans in solution. *Biochem. J.*, **173,** 103–114.

Scott,J.E., Heatley,F., Moorcroft,D. and Olavesen,A.H. (1981) Secondary structures of hyaluronate and chondroitin sulphates. *Biochem. J.*, **199,** 829–832.

Scott,J.E., Heatley,F. and Hull,W.E. (1984) Secondary structure of hyaluronate in solution. *Biochem. J.*, **220,** 197–205.

Scott,J.E., Cummings,C., Brass,A. and Chen,Y. (1991) Secondary and tertiary structures of hyaluronan in aqueous solution, investigated by rotary shadowing-electron microscopy and computer simulation. *Biochem. J.*, **274,** 699–705.

Sheehan,J. K., and Atkins,E.D.T. (1983) X-Ray fiber diffraction study of the conformational changes in hyaluronate induced in the presence of sodium, potassium and calcium cations. *Int J. Biol. Macromol.*, **5,** 215–221.

Sheehan,J.K., Gardner,K.H. and Atkins,E.D.T. (1977) Hyaluronic acid: a double-helical structure in the presence of potassium at low pH and found also with the cations ammonium, rubidium and caesium. *J. Mol. Biol.*, **117,** 113–135.

Sicinska,W. and Lerner,L.E. (1996) A detailed ^{1}H and ^{13}C NMR study of a repeating disaccharide of hyaluronan: the effect of sodium and calcium ions. *Carbohydr. Res.*, **286,** 151–159.

Sicinska,W., Adams,B. and Lerner,L.E. (1993) A detailed ^{1}H and ^{13}C NMR study of a repeating disaccharide of hyaluronan: the effects of temperature and counterion type. *Carbohydr. Res.*, **242,** 29–51.

Steinbach,P.J. and Brooks,B.R. (1994) New spherical cut-off methods for long range forces in macromolecular simulation. *J. Comp. Chem.*, **15,** 667–683.

Thogersen,H., Lemieux,R.U., Bock,K. and Meyer,B. (1982) Justification for the exo-anomeric effect. conformational analysis based on nuclear magnetic resonance spectroscopy of oligosaccharides. *Can. J. Chem.*, **60,** 44.

Tvaroska,I. and Tomas,B. (1989). Anomeric and exo-anomeric effects in carbohydrate chemistry. *Adv. Carbohydr. Chem. Biochem.*, **47,** 45–123.

Ueda,K. and Brady,J.W. (1996) The effect of hydration upon the conformation and dynamics of neocarrabiose, a repeat unit of α-carrageenan. *Biopolymers*, **38,** 461–469.

van Gunsteren,W.F., and Berendsen,H.J.C. (1977) Algorithms for macromolecular dynamics and constraint dynamics. *Mol. Phys.*, **34,** 1311–1327.

Verlet,L. (1967) Computer experiments on classical fluids. I. Thermodynamical properties of Lennard-Jones molecules. *Phys. Rev.*, **159,** 98–103.

Winter,W.T. and Smith,P.J.C. (1975) Hyaluronic acid: structure of a fully extended 3-fold helical sodium salt and comparison with the less extended 4-fold helical forms. *J. Mol. Biol.*, **99,** 219–235.

Received on October 18, 1996; revised on January 7, 1997; accepted on January 13, 1997